Effective temperatures, sawtooth mixing, and stochastic diffusion ripple loss of fast H+ minority ions driven by ion cyclotron heating in the Tokamak Fusion Test Reactor

M. P. Petrov, R. Bell, R. V. Budny, N. N. Gorelenkov, S. S. Medley et al.

Citation: Phys. Plasmas **6**, 2430 (1999); doi: 10.1063/1.873539
View online: http://dx.doi.org/10.1063/1.873539
View Table of Contents: http://pop.aip.org/resource/1/PHPAEN/v6/i6
Published by the AIP Publishing LLC.

Effective temperatures, sawtooth mixing, and stochastic diffusion ripple loss of fast H^+ minority ions driven by ion cyclotron heating in the Tokamak Fusion Test Reactor

M. P. Petrov,[a] R. Bell, R. V. Budny, N. N. Gorelenkov,[b] S. S. Medley, R. B. White, and S. J. Zweben
Princeton Plasma Physics Laboratory, P.O. Box 451, Princeton, New Jersey 08543

(Received 29 July 1998; accepted 23 February 1999)

This paper presents studies of the H^+ minority ions driven by Ion Cyclotron Radio Frequency (ICRF) heating in the Tokamak Fusion Test Reactor (TFTR) [R. J. Hawryluk *et al.*, Phys. Plasmas **5**, 1577 (1998)] deuterium plasmas using primarily passive H° flux detection in the energy range of 0.2–1.0 MeV. The measured passive H^+ energy spectra are compared with active (Li pellet charge exchange) results. It is shown that in the passive mode the main donors for the neutralization of H^+ ions in this energy range are C^{5+} ions. The measured effective H^+ tail temperatures range from 0.15 MeV at an ICRF power of 2 MW to 0.35 MeV at 6 MW. Radial redistribution of ICRF-driven H^+ ions was detected when giant sawtooth crashes occurred during the ICRF heating. The redistribution affected ions with energy below 0.7–0.8 MeV. The sawtooth crashes displaces H^+ ions outward along the plasma major radius into the stochastic ripple diffusion domain where those ions are lost in ~10 msec. These observations are consistent with the model of the redistribution of energetic particles developed previously to explain the results of deuterium-tritium (DT) alpha-particle redistribution due to sawtooth oscillations observed in TFTR. The experimental data are also consistent with numerical simulations of H^+ stochastic ripple diffusion losses. © *1999 American Institute of Physics.*

I. INTRODUCTION

Studies of the H^+ minority ions driven by Ion Cyclotron Radio Frequency (ICRF) heating in the Tokamak Fusion Test Reactor (TFTR)[1] deuterium plasmas were performed using neutral particle analysis in the energy range of 0.2–1 MeV. The neutral particle measurements were obtained using a high energy Neutral Particle Analyzer (NPA) developed by the Ioffe Physical-Technical Institute.[2] Similar measurements were performed earlier on the Joint European Torus (JET),[3] where efficient passive neutralization of MeV energy protons was first observed in the plasma core.[4] The main donors for the neutralization of the protons appeared to be the hydrogen-like low Z impurity ions. In a later paper,[5] a detailed analysis of the neutralization processes of MeV protons in JET was made, and the cross sections of the electron capture by H^+ ions from C^{5+} and Be^{3+} ions (the main donors in JET plasmas) were calculated. Similar measurements of the ICRF-driven H^+ minority have also been made on the Japanese tokamak, JT-60U.[6]

The high energy NPA was used on TFTR primarily for Pellet Charge Exchange (PCX) diagnostics,[7,8] wherein active charge exchange measurements of the energy and radial distributions of deuterium-tritium (DT) alpha particles were obtained in conjunction with impurity pellet injection. In parallel, passive measurements of H^+ ICRF-driven minority ions at energies up to the MeV range were also performed. The experimental data presented in this paper are mainly the results of operation in the passive pulse counting mode.[9] We present here the values of the H^+ effective temperatures and also the results of the studies of H^+ sawtooth mixing and stochastic diffusion ripple loss measured with the use of this technique.

II. PHYSICAL BASIS OF THE PASSIVE CHARGE-EXCHANGE DIAGNOSTIC

As was mentioned above, passive measurement of the ICRF-driven H^+ minority ions in the MeV energy range is based on electron capture by H^+ ions from hydrogen-like low-Z impurity ions. The most probable donors for electron capture in TFTR plasmas are C^{5+} ions because the main low-Z impurity was carbon. In principle, another possible donor could be the residual $D°$ atoms. The cross-sections for charge exchange of H^+ ions with $D°$ atoms[10] and C^{5+} impurity ions[5] are shown in Fig. 1. The charge-exchange rates of H^+ on $D°$ and C^{5+} are shown in Fig. 2. Here the density of C^{5+} in the plasma core is equal to 10^{10} cm^{-3} (estimated on the basis of spectroscopic measurements) and the upper limit of $D°$ density is estimated to be $\sim 10^8$ cm^{-3}. The energy range of the NPA measurements is also indicated. It is clearly seen from the figure that the dominant donor in TFTR plasmas in the energy range of the interest is C^{5+}. Therefore, we can conclude that the NPA detects the H° passive signal as a result of the reaction

$$H^+ + C^{5+} \rightarrow H° + C^{6+}. \quad (1)$$

[a]Permanent address: A. F. Ioffe Physical-Technical Institute, St. Petersburg, 194021, Russia.
[b]Permanent address: TRINITI, Troitsk, 142092, Russia.

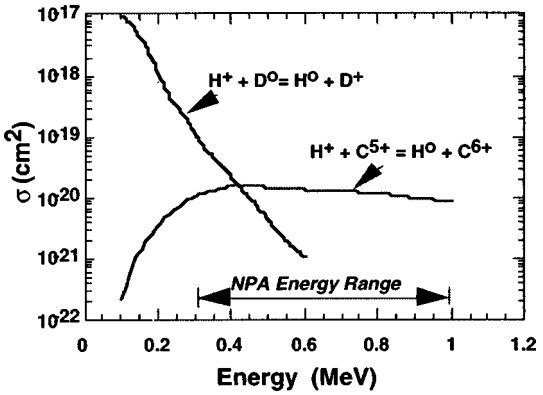

FIG. 1. Cross section for charge-exchange by protons with $D°$ atoms and with C^{5+} impurity ions.

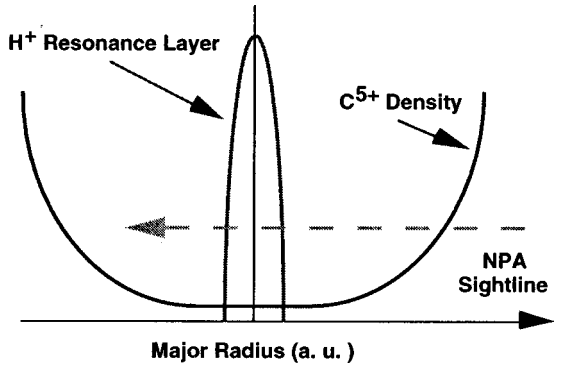

FIG. 3. Schematic illustrating passive H^+ diagnostic integration over the NPA sightline. Note that the H^+ energetic ion distribution to be measured is core-localized while the C^{5+} charge exchange donor is edge weighted.

The single-sightline NPA was located in the midplane with its line of sight at a toroidal angle of 2.75° relative to the major radius direction. Therefore, only deeply trapped ions with pitch angles in a narrow range $v_\parallel/v = -0.048 \pm 10^{-3}$ were detected. In the passive operating mode, the NPA count rate, $N_n(E)$, is related to the neutral flux at the analyzer, $\Gamma_{H°}$, through

$$N_n(E) \sim \eta(E) \Delta E_n \Gamma_{H°}, \tag{2}$$

where $\eta(E)$ is the calibrated NPA detection efficiency, ΔE_n is the energy width of the nth channel, and the units of $\Gamma_{H°}$ are $cm^{-2}\,s^{-1}\,eV^{-1}$. The neutral flux integrated over the PCX observation sight line can be related to the plasma parameters by

$$\Gamma_{H°} = \int N_{H^+}(l) N_{C^{5+}}(l) f_{H^+}(E,l) \sigma v_{H^+} \mu(E,l) dl, \tag{3}$$

where $N_{H^+}(l)$, $N_{C^{5+}}(l)$ are the profiles of H^+ and C^{5+} densities, $f_{H^+}(E,l)$, is the local H^+ energy distribution function, σ is the cross section of the $H^+ + C^{5+}$ reaction, v_{H^+} is the H^+ velocity, and $\mu(E,l)$ represents the plasma transparency for the detected H° atoms generated at a distance l from the plasma edge. This transparency is not a significant factor for the sub-MeV and MeV H° atoms being measured and has to be taken into account only for the low energy part of the PCX energy range shown in Figs. 1 and 2.

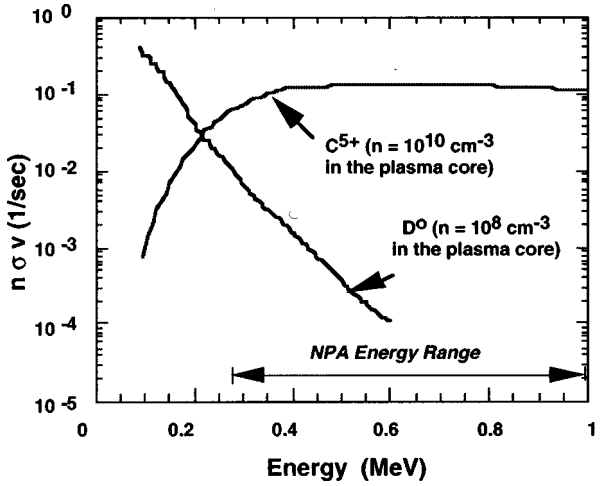

FIG. 2. Charge-exchange rates of H^+ ions with C^{5+} ($n = 10^{10}$ cm^{-3} in the TFTR plasma core) and with $D°$ ($n = 10^8$ cm^{-3} in the plasma core). The C^{5+} rate dominates at the higher H^+ energies of interest in the NPA measurements.

As shown schematically in Fig. 3, in the case of the core localized ICRF minority ion heating in TFTR, the $N_{H^+}(l) N_{C^{5+}}(l)$ value is constant (see Fig. 10 below) and the energy spectrum of H^+ ions, $f_{H^+}(E)$, averaged over the resonance layer, can be related to the NPA measurement by combining Eqs. (2) and (3) to give

$$f_{H^+}(E) \sim dn_{H^+}/dE \sim N_n(E) \{\sigma(E) v_{H^+} \mu(E,0)\, \eta(E) \Delta E_n\}^{-1}. \tag{4}$$

Active PCX measurements obtained with the use of the Li pellets injected into the plasma[8] were also used in some cases for measuring the H^+ tail distributions. In this case, H^+ ICRF-driven ions interacted with the lithium pellet ablation cloud to form an equilibrium neutral fraction, $F_0^\infty(E)$, as a result of the reaction

$$H^+ + Li^+ \rightarrow H° + Li^{2+}. \tag{5}$$

The energy distribution derived from PCX active signals can be expressed as

$$dn_{H^+}/dE \sim S_n(E) \{F_0^\infty(E) v_{H^+} \mu(E)\, \eta(E) \Delta E_n\}^{-1}, \tag{6}$$

where $S_n(E)$ is the measured PCX signal in the nth channel of the NPA in the current mode with units of volts and values of the neutral equilibrium fraction, $F_0^\infty(E)$, were taken from Ref. 8.

Figure 4 presents the active PCX signal versus pellet flight time for the NPA channel which detected H^+ ions of energy 0.72 MeV. This signal was taken during the ICRF fundamental on-axis heating of H^+ minority in a deuterium plasma (#96085, ICRF frequency 43 MHz, $B_T = 3.2$ Tesla, ICRF power 2.1 MW). On the horizontal axis, the radial position of the pellet is shown as derived from the measured pellet velocity (653 ms^{-1}). The contour of the signal measured by the PCX diagnostic corresponds to the radial position, shape, and width ($\Delta R = 6.1$ cm) of the H^+ resonance layer. The low level passive signal is also seen before and after the pellet signal.

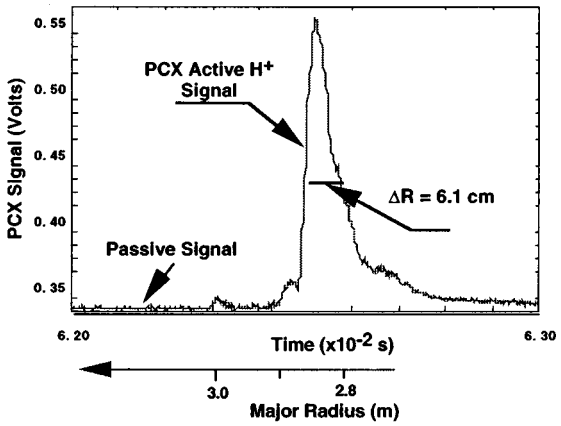

FIG. 4. The radial position and shape of the $H^+(E=0.72$ MeV) resonance measured by the PCX active diagnostic for fundamental H^+ ICRF heating in a TFTR deuterium plasma. Measurements from a look-down photodiode array are used to convert the pellet-induced active PCX signal from the time domain to radial position in the plasma.

Figure 5 shows the active energy spectrum of ICRF-driven H^+ ions for the discharge presented in Fig. 4 and the passive spectrum averaged over 100 ms during an ICRF power pulse in a discharge with the same parameters (#96080). It is seen that active and passive spectra have the same exponential shapes $dn_{H^+}/dE \sim \exp-(E/T_{\text{eff}})$ and very similar effective temperatures, T_{eff}. This provides additional evidence that the proper donor (C^{5+}) was chosen to derive the passive energy spectrum.

The passive measurements of H^+ ICRF-driven minority effective temperature in deuterium plasmas were performed routinely during ICRF runs on the TFTR. Figure 6 presents the effective temperature, $T_{\text{eff}}(H^+)$, of the H^+ minority versus ICRF power, P_{RF}, for a collection of 67 discharges. The measurements were made in deuterium on-axis, ICRF-heated discharges for the following range of plasma parameters: $I_{\text{plasma}}=(1.3–1.8)$ MA, $N_e(0)=(2.4–6.0)10^{13}$ cm^{-3} and $T_e(0)=(2.6–10)$ keV. It can be seen that $T_{\text{eff}}(H^+)$ increased monotonically with P_{RF} and in the range 0.8–6 MW changes from 0.12 to 0.34 MeV.

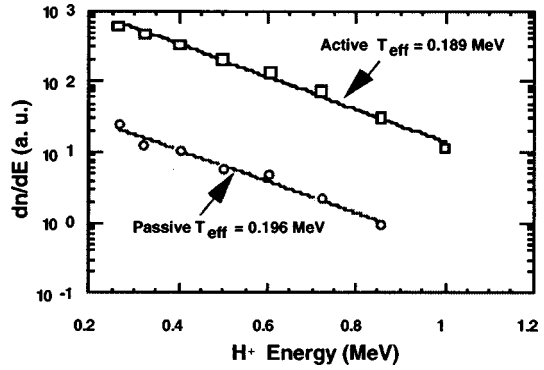

FIG. 5. Active and passive energy spectra of H^+ ICRF-driven minority ions in a TFTR deuterium plasma are in close agreement. Both discharges were obtained with on-axis heating at $P_{\text{ICRF}}=2.1$ MW, $F=43$ MHz, $n_e(0)=5.10^{13}$ cm^{-3}.

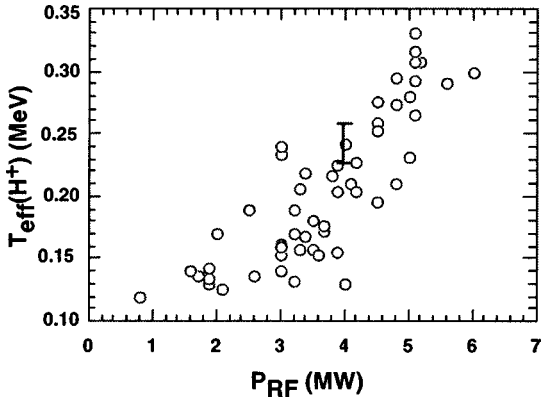

FIG. 6. H^+ effective temperatures, $T_{\text{eff}}(H^+)$, versus ICRF power (P_{RF}) for on-axis ICRF-heated deuterium plasmas in TFTR. The error in the $T_{\text{eff}}(H^+)$ measurements was typically 10%–15%.

III. SAWTOOTH MIXING OF ICRF-DRIVEN FAST H^+ IONS

A. Experimental observations

The effective temperatures, $T_{\text{eff}}(H^+)$, presented above, were measured in quiescent plasma in the absence of strong low-frequency magnetohydrodynamic (MHD) events like giant sawtooth crashes or disruptions. Now we will describe the behavior of the ICRF-driven H^+ minority ions in the presence of strong MHD events like a giant sawtooth crash in TFTR.

The influence of sawtooth oscillations on fast ions in tokamaks is of considerable interest because theoretical studies showed they can lead to a significant redistribution of ions.[11] The influence of sawtooth effects on injected neutral beam ions and fusion products in DD plasmas has been discussed elsewhere.[12,13] During DT experiments on TFTR, the PCX diagnostic revealed strong redistribution of trapped MeV alpha particles radially outward well beyond the $q=1$ surface after sawtooth crashes.[14–16]

Figure 7 presents the signals for H^+ ions (0.266 MeV) and x-rays showing two giant sawtooth crashes and the signal of lost H^+ ions measured by the lost alpha detector[17] located 60° below the outer midplane on the wall of the vacuum vessel. The bottom panel is the signal indicating Toroidal Alfvén Eigenmode (TAE) modes in the range of 150–200 kHz measured with the Mirnov coils. These modes are induced by the generation of ICRF-driven H^+ high energy tails. This phenomenon is described in detail elsewhere.[18] We see here that at the time of giant sawtooth crashes, dramatic increases of the 0.266 MeV H^+ signal occur along with sharp spikes on the H^+ lost ions. We note that the lost ion signal is averaged over the pitch angle range 45–83° and an H^+ energy range 0.4–2 MeV. It is interesting that rather strong TAE activity does not appear to directly affect the measured H^+ signal of the deeply trapped ions.

Figure 8 presents the H^+ signal taken from the 1st, 3rd, and 7th channels of the NPA detecting H^+ at energies of 0.266, 0.404, and 0.855 MeV. It is seen that the influence of the crashes on the signal diminishes with increasing of H^+ energy and completely disappears at an H^+ energy of 0.855

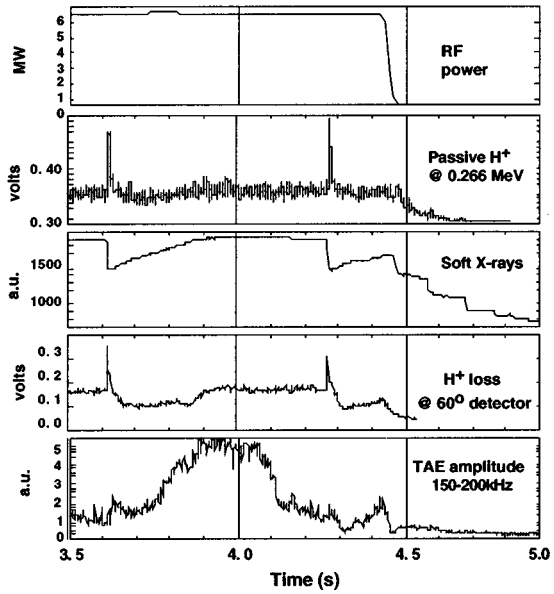

FIG. 7. Shown is the time history of a discharge with ICRF-driven H^+ minority heating including: ICRF power, passive H^+ signal (0.266 MeV), soft x-ray signal showing two giant sawtooth crashes, tail loss rate at the 60° lost alpha detector, and a Mirnov signal exhibiting the ICRF tail ion driven TAE.

MeV. The time decay of the spikes in the 1st and 3rd channels is a few milliseconds.

The schematic presented in Fig. 9 illustrates the qualitative model which we propose to explain detected H^+ spikes in the presence of sawtooth crashes and their subsequent time decay. The H^+ resonance layer shown here is located near the plasma center. Immediately after the crash, H^+ ions can be redistributed and moved outward (the H^+ mixing radius, r_{mix}, is shown). The C^{5+} radial density profile has the shape shown in Fig. 9 (the C^{5+} density increases near the plasma periphery). If r_{mix} is large enough to reach the region with increasing C^{5+} density, a sharp increase of H^+ signal will occur. The stochastic ripple diffusion domain is located in the outer region of the tokamak plasma where fast H^+ ions will be lost in a few milliseconds.[19] The expected position of the stochastic domain for sub-MeV H^+ ions is shown on the

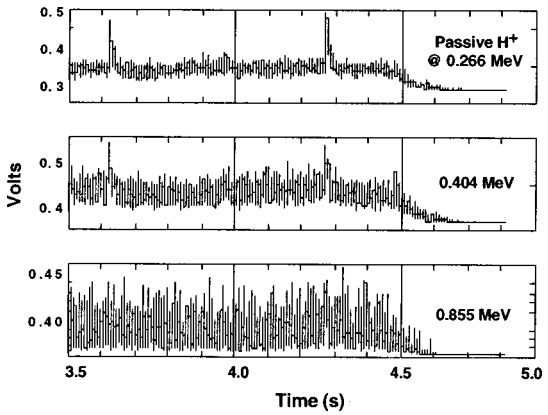

FIG. 8. Passive signals for ICRF-driven H^+ minority ions of different energies in the presence of two giant sawtooth crashes (the same discharge as Fig. 7).

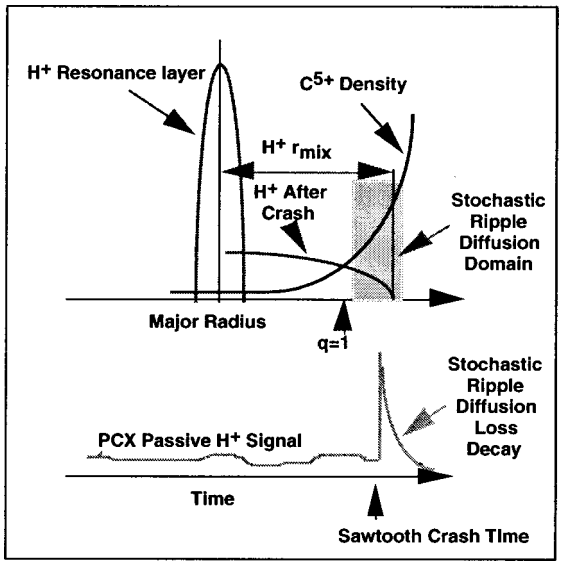

FIG. 9. Schematic illustrating the origin of the H^+ passive charge exchange signal generated by H^+ sawtooth mixing.

schematic. The poor confinement of the H^+ ions displaced by the sawtooth crash into the stochastic domain leads to the detected decay of the signal. This scenario is also consistent with the signals for lost H^+ ions (see Fig. 7). It is seen that the time decay of the lost ion signal is very close to that of the H^+ passive charge exchange signal. Outward of the stochastic domain there is the region of prompt losses. Losses of this kind are also seen on the lost H^+ signal. We see here very sharp spikes (prompt losses) and delayed losses corresponding to the stochastic ripple diffusion. Below, this model will be presented quantitatively.

B. Modeling of ICRF-driven H^+ sawtooth mixing in TFTR

We have mentioned above that during DT experiments on TFTR the redistribution of alpha particles due to sawtooth crashes was observed. To explain the redistribution, a model of alpha sawtooth mixing was developed[20] based on the fast particle orbit averaged toroidal drift in a perturbed helical electric field generated by the sawtooth crash with an adjustable absolute value. Such a drift of fast particles results in a change of their energy and a redistribution in phase space. This model agreed well with the measured alpha-particle redistribution due to sawtooth mixing.[14,15]

In this paper, the model is applied to ICRF-driven H^+ ions to describe the experimentally measured H^+ redistribution presented above. The results of the H^+ redistribution modeling are shown in Fig. 10. Here we see the ICRF H^+ precrash resonance contours for the energies 0.25, 0.5, and 0.75 MeV located in the TFTR plasma core. An initial precrash distribution function was chosen as exponential in energy with effective temperature $T_{\mathrm{eff}}(H^+)=269$ keV (in accordance with the measurements) and Gaussian in pitch angle, so that H^+ ions are localized near the ICRH resonance layer. The resonance location is taken from the frequency

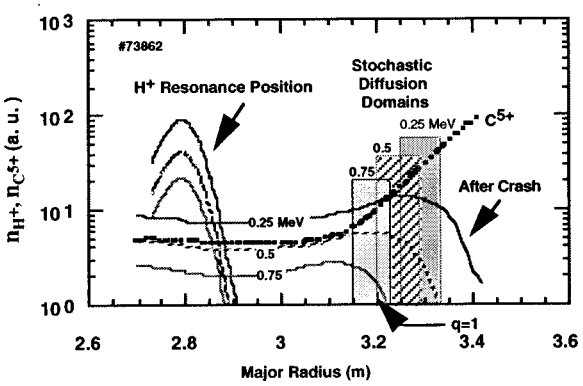

FIG. 10. Modeling results are shown for the ICRF-driven H^+ ion sawtooth mixing. Three H^+ energies (0.25, 0.50, and 0.75 MeV) are presented before and after the sawtooth crash. Adjustable parameters used in the modeling were $E_{\rm crit}=317$ keV, $E_e=1.4$ kV/cm and $\tau_{pr}=\tau_{cr}=50$ μs. The radial locations of the stochastic ripple domains for the noted H^+ energies are shown by the hatched regions. The dotted line is the C^{5+} radial density distribution.

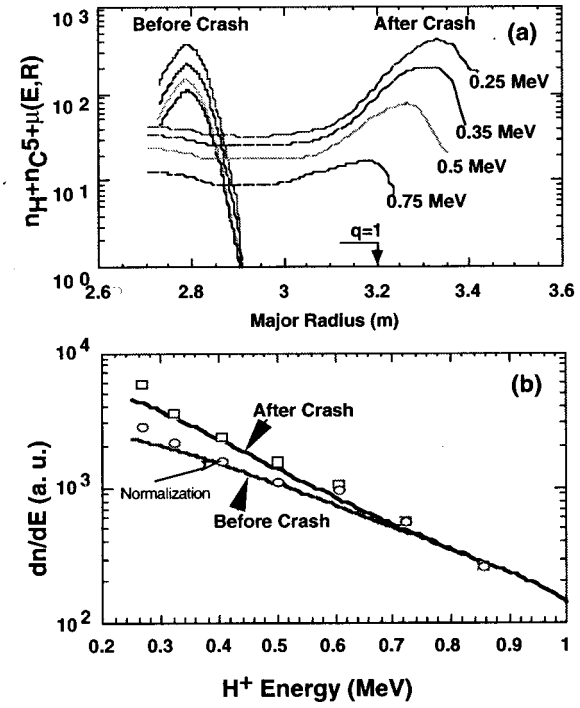

FIG. 11. Shown are (a) the emissivity, $n_{\rm H^+}n_{\rm C^{5+}}\mu(E,R)$, of the $H^+ + C^{5+}$ reaction before and after the sawtooth crash versus major radius, and (b) the energy spectra before and after the crash integrated over the observation line (major radius) on the basis of the presented emissivity. Solid lines are model results and data points are passive experimental spectra before and after the crash.

and toroidal field values. The width of the resonance is taken to be 10 cm. Plasma equilibrium and other parameters were taken from the TRANSP code.[21]

The model predictions of the redistribution after the crash are also shown in Fig. 10. The mixing radius used for modeling was determined from the Kadomtsev reconnection model[22] on the basis of q profiles from the TRANSP code. The model shows that the mixing radius and the number of particles involved in the redistribution decrease with increasing energy. This is consistent with the experimental data presented in Fig. 8. The relative C^{5+} radial density profile is also shown as derived from multichord spectroscopic measurements of the C^{5+} line at 5291 Å. The radial distribution of the brightness of the C^{5+} line integrated over the observation line has been transformed using Abel inversion to obtain the emissivity (radial distribution of the intensity of this line). The relative C^{5+} density profile has been calculated by the dividing of the emissivity by the local electron density of the plasma. The dependence of the emissivity on the variation of electron temperature with major radius was assumed to be negligible for plasma electron temperatures in the range of 1.5 ± 1.0 keV.

To normalize the model calculations to the experimental data, the emissivity distribution of the reaction $H^+ + C^{5+} \rightarrow H° + C^{6+}$ (i.e., the H° source function) over the major radius was calculated and the results for different energies of H^+ ions are presented in Fig. 11(a). The vertical axis of the plot is the product of H^+ density, C^{5+} density, and plasma transparency $\mu(E,R)$. The values of $\mathbf{n}_{\rm H^+}$ and $\mathbf{n}_{\rm C^{5+}}$ are taken from Fig. 10. The passive experimental spectra for the period before the crash (circles) and after the crash (squares) are shown in Fig. 11(b). Note that the spectrum before the crash consists of the signals coming from the resonance at the plasma center only, whereas the signals after the crash come from both the resonance region and the redistributed H^+ ions. The model spectra (solid lines) are the results of integration over the major radius of the emissivity multiplied by the transparency, $\mu(E)$, for the noted H^+ energies. The model and experimental spectra are normalized at one point. To obtain agreement between the model and the experimental data, it was necessary to use the adjustable parameter $E_{\rm crit}=317$ keV which corresponds with $\tau_{\rm crash}=50$ μs and a helical electric field $E_e=1.4$ kV/cm in the model. Here $E_{\rm crit}$ is an adjustable critical energy which is equal to the energy of the particles having toroidal precession time equal to the crash time. Note that according to Ref. 20, particles with $E>E_{\rm crit}$ average the effect of the electric field during the toroidal precession and are less affected by the crash than particles with the energy $E<E_{\rm crit}$. Comparing the experimental and calculated energy spectra shown in Fig. 11(b), we can conclude that the mixing model is in good agreement with the experimental data when reasonable values of adjustable parameters are assumed.

Our understanding of the mechanism for generation of the H^+ signals observed in the presence of the sawtooth crashes is illustrated well by the data presented in Fig. 12. Here the time history of a TFTR discharge with ICRF-driven H^+ minority ions and with a short $D°$ neutral beam pulse is shown. The H^+ signal spikes generated by the giant sawtooth crash are seen as well as the signal increase during the neutral beam (NB) blip. The H^+ signal due to the crash decrease with increasing H^+ energy in accordance with the model described above. The relative level of H^+ signals in the presence of the NB blip remains approximately constant for all measured energies. Note that on TFTR the NPA observation line does not directly view any of the heating beams injected into the plasma. Therefore the signal cannot be the result of direct charge-exchange of H^+ ions with the $D°$ atoms of the

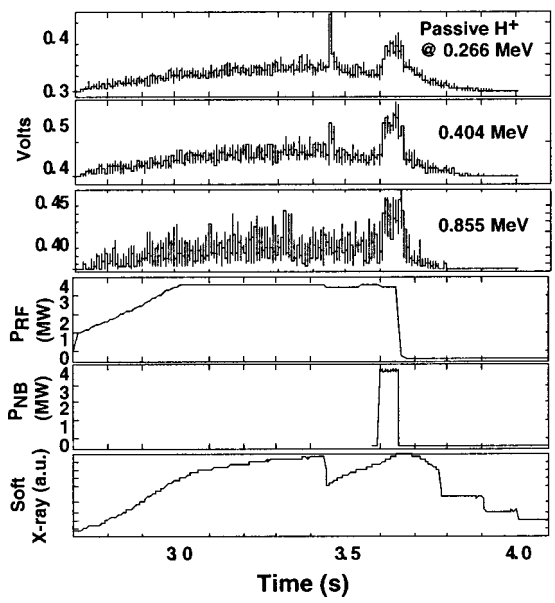

FIG. 12. The time history of a discharge with ICRF-driven H^+ minority ions and a D° neutral beam blip are shown, including passive H^+ signals (0.266, 0.404, 0.855 MeV), ICRF power, NB power, and a soft x-ray signal indicating giant sawtooth crashes.

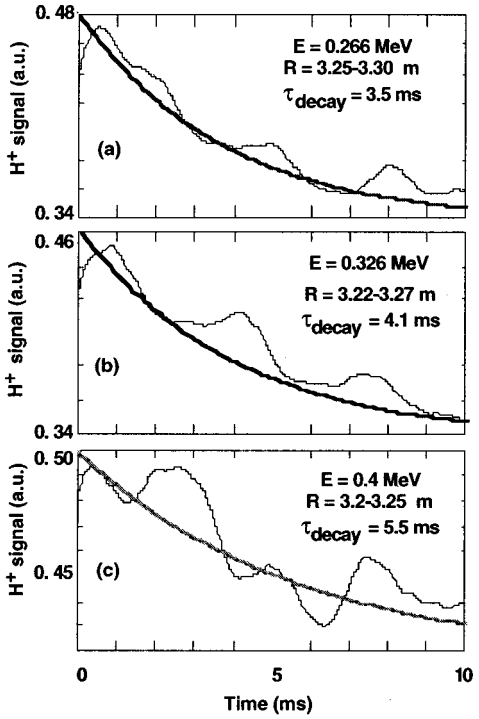

FIG. 13. The decay of the experimental H^+ signal after the giant sawtooth crash and the ORBIT code simulations of this decay, τ_{decay}, due to stochastic ripple diffusion losses are shown for selected H^+ energies.

beam. The origin of this signal is described in detail elsewhere.[4] According to this paper, the heating beams injected into the tokamak plasma change the ionization balance of the carbon ions and lead to an increase of the C^{5+} density in the plasma core because of the increasing probability for electron capture by C^{6+} ions from the beam. It was shown that in JET the injection of the heating beams leads to an increase of the C^{5+} density by a factor of 3–4 not only in the vicinity of the beams but all around the torus. The same phenomenon obviously occurs in TFTR. It is important to note that the decrease of the H^+ signal due to the crash with increasing H^+ energy and the complete absence of the signal above an energy 0.855 MeV (see Fig. 12) is evidence that there are no significant changes in the C^{5+} population in the plasma core during the sawtooth crash.

IV. STOCHASTIC RIPPLE DIFFUSION LOSSES OF ICRF-DRIVEN H^+ IONS DUE TO SAWTOOTH MIXING

To simulate the H^+ minority confinement in the TFTR plasma after a sawtooth crash, we used the ORBIT[23–25] guiding center code. In the ORBIT code, particle motion is calculated in toroidal magnetic geometry using a computed equilibrium and ripple magnetic fields. The effects of slowing down and pitch angle scattering in calculating the stochastic ripple diffusion are included, which gives rise to diffusion from the nonstochastic domain to the stochastic domain. Figure 10 presents the locations of the stochastic diffusion domains calculated with the ORBIT code for specific energies (0.25, 0.5, and 0.75 MeV) and for the experimental pitch-angle, $v_\parallel/v = -0.048$. The ORBIT code predicts that the ions whose banana tips are located inside these domains are lost in a few milliseconds because of the stochastic ripple diffusion. Just outboard of these domains is the region of much faster stochastic losses, which occur during a few bounce periods. Farther outward is the region of prompt first orbit loss. It is seen from Fig. 10 that the TFTR ICRF-driven trapped H^+ ions are transported outward after the giant sawtooth crash, and reach the stochastic domains. A fraction of the ions can pass through these domains and even reach the prompt loss region.

For more detailed analysis of the H^+ confinement time inside the stochastic domains, 5000 particles with energies of 0.266, 0.322, and 0.4 MeV were followed. The results of this analysis are presented in Fig. 13. Here the light curves are smoothed experimental H^+ signals which occur immediately after the crash (crash occurs at zero time). The solid lines show ORBIT code simulations of the H^+ decay due to the stochastic ripple diffusion losses. In the model, the initial radial distributions of the minority ions were chosen to represent the population of H^+ minority ions giving the maximum contribution to the H^+ signal [i.e., the maximum of the emissivity for each measured H^+ energy shown in Fig. 11(a)]. The initial radial location of the H^+ ions is indicated in the legend of Fig. 13. We used a uniform distribution in space and pitch angle so that the bounce point was at a major radius ranging from 3.2 to 3.3 m, with the vertical coordinate $Z=0$–0.30 m. The results show that the minority ions of interest are all lost after ~10–12 ms and their density evolution may be given roughly by the expression $n(H^+) = n_0 H^+) \exp(-t/\tau_{st})$, where τ_{st} is equal to 3.5, 4.1, and 5.5 ms for the specified H^+ energies. The confinement time of H^+ ions increases with increasing energy because the signals for ions with higher energies originate from deeper regions in the plasma where the influence of the stochastic ripple diffusion is weaker. It is seen that the ORBIT results are in a

good agreement with the experimental data. This result corroborates the model[20] used for sawtooth mixing of fast particles, since an incorrect H^+ post sawtooth distribution in major radius will change the computed decay time and spoil the observed agreement.

Above we discussed the influence of giant sawteeth ($\Delta T_e/T_e \sim 30\%$) on H^+ ions. We note that with smaller periodic sawtooth oscillations ($\Delta T_e/T_e \sim 10\%-15\%$), there are no changes in either the passive charge-exchange H^+ signal or the lost H^+ ion signal. This means that in this case the H^+ mixing radius is much smaller than in the case of the giant sawteeth. If we will assume that the C^{5+} density distribution in this plasma is similar to those shown in Fig. 10, we can conclude that the H^+ mixing radius in this case is less than 30–35 cm. Therefore the smaller sawteeth do not lead to sufficient H^+ redistribution to produce noticeable stochastic ripple diffusion losses.

V. CONCLUSIONS

Measurements of ICRF-heated H^+ ions in deuterium plasmas in TFTR based on the use of neutral particle analysis in the MeV energy range can provide important information on their effective temperature and their behavior in the presence of the MHD events.

It was shown that strong, low frequency MHD events like giant sawtooth crashes ($\Delta T_e/T_e \sim 30\%$) which occur during ICRF heating cause a strong redistribution of H^+ ions outward along the major radius. This redistribution leads to stochastic ripple diffusion loss of H^+ ions. This does not occur in smaller periodic sawtooth oscillations where $\Delta T_e/T_e \sim 10\%-15\%$. The observations are consistent with a model for the redistribution of energetic particles developed earlier to explain the results of DT alpha-particle redistribution due to sawtooth crashes that were observed on TFTR, and also with ORBIT code simulation of H^+ stochastic diffusion ripple losses.

ACKNOWLEDGMENT

This work was supported by U.S. Department of Energy Contract No. DE-AC02-76CH03073.

[1] M. G. Bell, S. Batha, M. Beer *et al.*, Phys. Plasmas **4**, 1714 (1997).
[2] A. I. Kislyakov, A. V. Khudoleev, S. S. Kozlovskij, and M. P. Petrov, Fusion Eng. Des. **34–35**, 107 (1997).
[3] A. Gibson and the JET Team, Phys. Plasmas **5**, 1839 (1998).
[4] M. P. Petrov, V. I. Afanassiev, S. Corti, A. Gondhalekar, A. V. Khudoleev, A. A. Korotkov, and A. C. Mass, in *Proceedings of the 1992 International Conference on Plasma Physics*, Innsbruck, 1992 (European Physical Society, Petit-Lancy, 1992), Vol. II, p. 1031.
[5] A. A. Korotkov, A. Gondhalekar, and A. J. Stuart, Nucl. Fusion **37**, 35 (1997).
[6] V. I. Afanassiev, Y. Kusama, M. Nemoto *et al.*, Plasma Phys. Controlled Fusion **39**, 1509 (1997).
[7] R. K. Fisher, J. M. McChesney, P. B. Parks *et al.*, Phys. Rev. Lett. **75**, 846 (1995).
[8] S. S. Medley, D. K. Mansfield, A. L. Roquemore *et al.*, Rev. Sci. Instrum. **67**, 3122 (1996).
[9] S. S. Medley, M. P. Petrov, A. L. Roquemore, and R. K. Fisher, Rev. Sci. Instrum. **70**, 841 (1999).
[10] J. E. Bayfield, Phys. Rev. **185**, 105 (1969).
[11] Ya. I. Kolesnichenko and Yu. V. Yakovenko, Nucl. Fusion **36**, 159 (1996).
[12] F. B. Marcus, J. M. Adams, D. S. Bond *et al.*, Nucl. Fusion **34**, 687 (1994).
[13] H. H. Duong and W. W. Heidbrink, Nucl. Fusion **33**, 211 (1993).
[14] M. P. Petrov, R. V. Budny, H. H. Duong *et al.*, Nucl. Fusion **35**, 1437 (1995).
[15] M. P. Petrov, N. N. Gorelenkov, R. V. Budny *et al.*, in *Fusion Energy: Proceedings of the 16th International Fusion Energy Conference*, Montreal, 1996 (International Atomic Energy Agency, Vienna, 1997), Vol. 1, p. 261.
[16] S. S. Medley, R. V. Budny, H. H. Duong *et al.*, Nucl. Fusion **38**, 1283 (1998).
[17] D. S. Darrow, S. J. Zweben, Z. Chang *et al.*, Nucl. Fusion **37**, 939 (1997).
[18] K. L. Wong, R. Majeski, M. Petrov *et al.*, Phys. Plasmas **4**, 393 (1997).
[19] R. L. Boivin, S. J. Zweben, and R. B. White, Nucl. Fusion **33**, 449 (1993).
[20] N. N. Gorelenkov, R. V. Budny, H. H. Duong, R. K. Fisher, S. S. Medley, M. P. Petrov, and M. H. Redi, Nucl. Fusion **37**, 1053 (1997).
[21] R. V. Budny, M. G. Bell, A. C. Janos *et al.*, Nucl. Fusion **35**, 1497 (1995).
[22] B. B. Kadomtsev, Sov. J. Plasma Phys. **1**, 389 (1975).
[23] R. B. White and M. S. Chance, Phys. Fluids **27**, 2455 (1984).
[24] R. B. White, Phys. Fluids B **2**, 845 (1990).
[25] R. B. White, R. J. Goldston, M. H. Redi, and R. V. Budny, Phys. Plasmas **3**, 3043 (1996).